3. V. E. Neuvazhaev, "Gas motion with given spatial distribution of pressure," Prikl. Mat. Mekh., 34, No. 1 (1970).

EXPERIMENTAL STUDY OF STRONG SHOCK PROPAGATION IN A CHANNEL

A. A. Kon'kov and A. I. Sokolov

UDC 533.6.011.72

The widespread use of shock tubes in laboratory practice is well known. However, despite existing information [1] about shock-wave velocities of ~ 100 km/sec, experimental data on the size of the shock-heated region behind the shock front are confined to the Mach numbers M = 10 [2]. Theoretical data do not go beyond the limit of this range except for air where calculations were performed up to M ≈ 20 [3, 4]. Behind strong shocks, the effects resulting from viscosity, thermal conductivity, and radiation of the medium should lead to serious deviation of the actual flow from the idealized pattern for uniform motion of a piston in a channel filled with a nonviscous, thermally nonconducting, and nonradiating medium. It is therefore practical to make an experimental study of the behavior of density and of the size of the shock-heated region behind a shock front propagating down the channel of a shock tube that is capable of producing velocities up to 8 km/sec.

The shock tube used in the experiments was similar to the one described in [5], but in these experiments the internal cross section of the channel in the low-pressure chamber was a 27 × 27 mm^2. An additional section of greater cross section was installed beyond the viewing ports so that reflection of the shock wave from the end did not disturb the flow patterns. Argon was used as the test gas.

The study was based on the interferometric method for determination of density using the Rozhdestvenskii system [6] in which a Mach–Zender interferometer was crossed with a spectrograph. This system was supplemented with a time sweep similar to that used in [7]. The experimental arrangement is shown in Fig. 1. In the figure, I-IV are interferometer mirrors; L_1 and L_2 are lenses; 6 is an ISP-51 spectrograph; 7 and 8 are a driven photodetector and its supply unit; 5 and 4 are the light source and its supply unit.

A pulsed discharge in a capillary was used as the probing light source 5; the energy distribution in its spectrum corresponded to the distribution in a black-body spectrum at a temperature of approximately 40,000°K. A description of this source is given in [8].

The system for velocity measurement is shown schematically in Fig. 1. Here D_1, D_2, D_3, D_4, and D_5 are ionization detectors with the distances D_1D_2, D_2D_3, D_3D_4, and D_4D_5 being respectively, 100, 300, 80, and 240 mm; 1 is a unit which produces an electrical impulse after shorting of the interelectrode gaps of the ionization detectors by plasma; 2 is an S1-17 oscilloscope; 3 is a G-4-18A sine-wave generator; 4 is a synchronization unit.

The driven photodetector consisted of an objective, a 12-sided prism with mirror faces, and a film cassette (Isopankhrom-13 film was ususally used). The rate of prism rotation during an experiment was 375 rps, which made it possible to obtain a time resolution of about 0.3 μsec. Since high-order interference was used, nearly vertical bands were produced on the film. When one of the arms of the interferometer was crossed by a wave or by the contact region, a shift in the interference pattern occurred. Detection of these points in time on the film made it possible to determine the distance between the shock wave and the contact region.

Moscow. Translated from Zhurnal Prikladnoi Mekhaniki i Tekhnicheskoi Fiziki, No. 4, pp. 23-28, July-August, 1976. Original article submitted July 21, 1975.

This material is protected by copyright registered in the name of Plenum Publishing Corporation, 227 West 17th Street, New York, N.Y. 10011. No part of this publication may be reproduced, stored in a retrieval system, or transmitted, in any form or by any means, electronic, mechanical, photocopying, microfilming, recording or otherwise, without written permission of the publisher. A copy of this article is available from the publisher for $7.50.

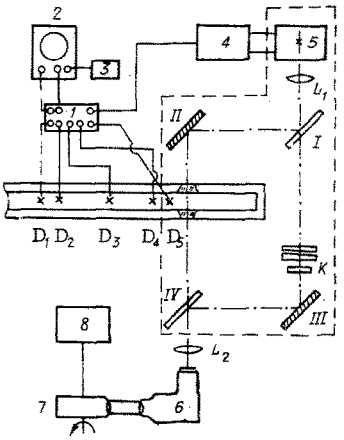

Fig. 1

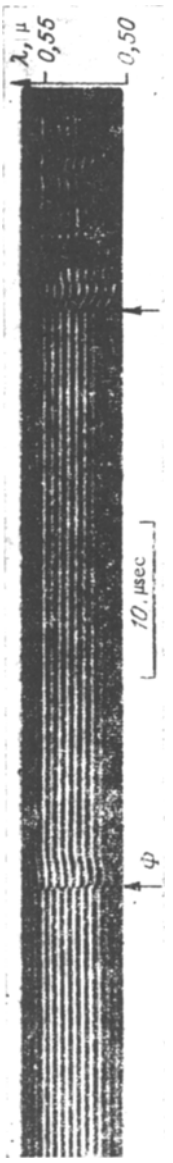

Fig. 2

The distance from the second diaphragm to the center of the window in the measuring section was 220 cm. This value was selected on the basis that the length of the shock-heated region in the case of a turbulent layer practically reaches its maximum value at 80-90 channel diameters from the diaphragm [3]. For the analogous situation to occur with laminar flow, it is necessary to increase this distance by factors of 2-3, which is inconvenient because it leads to a significant reduction in the shock-wave velocity in the section where the measurements are made.

An interferogram obtained for shock-wave motion in argon (initial pressure, 10 mm Hg) at a velocity of 4.3 km/sec is shown in Fig. 2 where it is apparent that after the abrupt displacement of the bands at Φ, which is associated with the shock front, there follows a region of density variation corresponding to the return of the medium to equilibrium (relaxation region). There then follows a region where further displacement of the interference bands is almost unobservable, i.e., the density remains practically unchanged. Beyond the region of stable bands, there follows a region of random variations in the interference pattern, the beginning of which is identified with the arrival of the contact region. The interval between the first abrupt shift in the interference pattern and the beginning of the random oscillations of the interference bands was taken as the duration of the shock-heated region. This time multiplied by the shock-wave velocity gives the size of the shock-heated region. As the shock-wave velocity increases, the relaxation region decreases, the bands in the interference pattern begin to experience a tilt that is small at first and then considerable, and the length of the shock-heated region decreases and is 1.5-2 cm at velocities of 7-8 km/sec. At such high velocities, intense radiation is produced

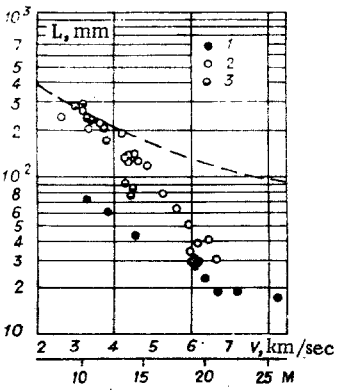

Fig. 3

behind the shock front which hinders the study of the behavior of interference bands for approximately 1 μsec after their first abrupt shift. Measured sizes of the shock-heated region in argon at 220 cm from the diaphragm are plotted in Fig. 3. The size of the shock-heated region is plotted on the ordinate; the shock velocity and the corresponding value of the Mach number are plotted along the abscissa; 1 denotes the results obtained for an initial pressure of 1 mm Hg, 2 for 10 mm Hg, and 3 for 50 mm Hg. The dashed line in Fig. 3 was calculated for an initial pressure of 10 mm Hg by means of the "contamination law" [9] according to which the length of the shock-heated region is reduced by a factor of two (because of mixing at the boundary of the contact region) in comparision with the length calculated without consideration of boundary layers and mixing. This relation was established for low Mach numbers and, as is clear from a comparison of the dashed curved and the experimental data for initial pressures of 10 and 50 mm Hg, the results of [9] and the experimental data agree in the region of Mach numbers M = 10-12. For initial pressures of 1 mm Hg over the entire range of Mach numbers covered, and also for 10 and 50 mm Hg when M > 15, the actual values for the length of the shock-heated region are considerably less than follows from the "contamination law" with the experimental values for the length of the shock-heated region differing by factors of approximately 5-6 for velocities around 8 km/sec [9]. Calculations performed in [3, 4] up to M = 10 assumed the validity of the Sutherland viscosity law with the ratio of the specific heat capacities being taken as 5/3 and the Prandtl number as 0.67. Since the fulfillment of these assumptions is doubtful at higher Mach numbers, it is inadvisable to extrapolate these curves into the region of higher Mach numbers for comparison with the results of this work.

In order to determine density, we select wavelengths $\lambda_1, \ldots, \lambda_n$ corresponding to the luminosity maxima before arrival of the shock wave. The number n is determined by the number of plasma components for which it is necessary to determine the concentration. The following relations are valid for these wavelengths:

a) before arrival of shock wave,

$$\sum_i r_{i0}(\lambda_1) N_{i0} = k_1\lambda_1/d, \ldots \sum_i r_{i0}(\lambda_n) N_{i0} = k_n \frac{\lambda_n}{d}; \tag{1}$$

b) after arrival of shock wave,

$$\sum_i r_{i0}(\lambda_1) N'_{i0} + \sum_j r_j(\lambda_1) N_j - r_e(\lambda_1) N_e = (k_1 + \delta_1) \frac{\lambda_1}{d}, \ \ldots$$

$$\sum_i r_{i0}(\lambda_n) N'_{i0} + \sum_j r_j(\lambda_n) N_j - r_e(\lambda_n) N_e = (k_1 + \delta_1) \frac{\lambda_n}{d}, \tag{2}$$

where $r_{i0}(\lambda)$, $r_j(\lambda)$, and $r_e(\lambda)$ are, respectively, the refraction of neutral, ionic, and electronic components per neutral particle, ion, or electron; N_{i0} and N'_{i0} are the concentrations of neutral particles before and after the arrival of the shock wave, respectively; N_j and N_e are, respectively, the ion and electron concentrations; $k_1, \ldots, k_n$ are the orders of interference including the shift resulting from the nonidentical arms of the interferometer; $\delta_1, \ldots, \delta_n$ are the shifts of the bands resulting from arrival of the shock wave; and d is the distance between the ports of the viewing section.

In writing the equation system (2), we assume that the contribution to refraction by excited particles differs little (per individual particle) from the contribution by the corresponding particles in the unexcited state.

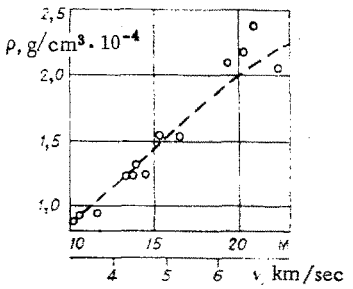

Fig. 4

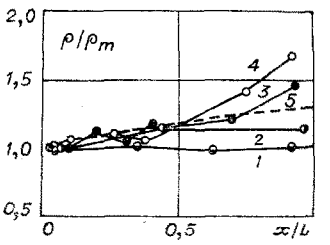

Fig. 5

When M ≈ 10, displacement of bands over the entire shock-heated region is practically absent and, consequently, the band shift caused by the effect of the boundary layer can be neglected. At higher Mach numbers, the size of the boundary layer decreases [3] and therefore its effect on displacement is not taken into consideration in writing the equation system (2).

Subtracting the first equation of the system (1) from the first equation of system (2), the second equation of system (1) from the second equation of system (2), etc., we obtain

$$\sum_i r_{i0}(\lambda_1)\Delta N_{i0} + \sum_j r_j(\lambda_1) N_j - r_e(\lambda_1) N_e = \delta_1 \frac{\lambda_1}{d}; \ldots$$
$$\sum_i r_{i0}(\lambda_n)\Delta N_{i0} + \sum_j r_j(\lambda_n) N_j - r_e(\lambda_n) N_e = \delta_n \frac{\lambda_n}{d}. \quad (3)$$

This system of equations makes it possible to determine N'_{i0}, N_j, and N_e if $r_{i0}(\lambda)$, $r_j(\lambda)$, and $r_e(\lambda)$ are known and $\delta_1, \ldots, \delta_n$ are assigned. For singly ionized argon, where the number of argon ions equals the number of electrons, we have from Eqs. (3),

$$r_0(\lambda_1)\Delta N_0 + [r_+(\lambda_1) - r_e(\lambda_1)]N_e = \delta_1\lambda_1/d;$$
$$r_0(\lambda_2)\Delta N_0 + [r_+(\lambda_2) - r_e(\lambda_2)]N_e = \delta_2\lambda_2/d. \quad (4)$$

The subscripts 0 and +, respectively, denote the argon atom and argon ion. According to [10, 11], $r_0(\lambda) = A \cdot (1 + B/\lambda^2)$, where $A = 1.04 \cdot 10^{-23}$, $B = 5.6 \cdot 10^{-3}$, and $r_e = e^2\lambda^2/2\pi mc^2$. One can assume $r_+(\lambda) = 0.69 r_0(\lambda)$ for the ionic component. The last relation was determined in [11] and confirmed in [12]. The specified constants and Eqs. (4) were used to determine the concentrations of atoms and ions. With a knowledge of these quantities, one can find the density. The error in the determination of the density by this method does not exceed 30%.

The band shift was determined in the following way. First the interference pattern was recorded for weak shock waves such that the band shift clearly did not exceed the spacing between bands. The shock-wave velocity was then increased gradually, which made it possible to follow the gradual change in the band shift and thereby determine δ. Integral and half-integral values of δ were used in the determination of density, since the determination of their locations on the wavelength scale can be performed with greatest accuracy.

Density values behind an incident wave propagating in argon at an intial pressure of 10 mm Hg determined by the method discussed are denoted by the circles in Fig. 4; the dashed curve is a calculated one in accordance with [13, 14]. The experimental values are related to the time immediately following the relaxation region. A comparison of the experimental and theoretical data leads to the conclusion that the actual values for argon density immediately behind a shock wave when M < 24 agree within experimental error with those calculated from conservation laws in the Rankine–Hugoniot form.

It appeared practical to follow the behavior of density over the entire shock-heated region by means of this method. Figure 5 shows the dependence of density on distance from the shock front in argon at an initial pressure of 10 mm Hg for the following Mach numbers: 1) M = 10.0; 2) M = 13.4; 3) M = 16.5; 4) M = 20.3; curve 5 from [16] is for M = 17. The ratio between the density in a given cross section of the shock-heated region and the minimum density in that region is plotted on the ordinate; the ratio between the distance from the shock front and the total length of the shock-heated region for a given Mach number obtained from the experimental data in Fig. 3 is plotted on the abscissa. The relaxation region is excluded from consideration. As is clear from Fig. 5, the density over the entire shock-heated region remains practically constant for Mach numbers up to 13.5 and can be calculated by means of conservation laws at the shock discontinuity. For Mach numbers M > 16, a similar statement can only be made with respect to the first half of the shock-heated region.

Subsequent increase in density becomes quite significant, goes beyond the limits of experimental error, and reaches 70%.

Calculations performed in [15] for a completely monatomic gas led to an increase of approximately 10% in all even for $M = \infty$ with the increase occurring mainly initially in a distance of roughly one-fifth of the shock-heated region. The changes in density observed experimentally, as seen in Fig. 5, were considerably greater and cannot be explained merely through the effect of the boundary layer. Radiation cooling can play a large part in this case and it is therefore reasonable to compare the experimental data with the calculations in [16, 17] where this effect was included. The consideration of radiation was performed more correctly in [16], since there, in contrast to [17], line radiation was taken into account. The comparison with the results of [16] is shown in Fig. 5. Note that [16] gives the temperature distribution calculated under the assumption of constant pressure behind the shock front. Using this assumption, one can convert from temperature distribution to density distribution. Curve 5 in Fig. 5 was obtained by such a conversion for $M = 17$. Comparison of this curve with curve 3, which was obtained for similar conditions, indicates satisfactory agreement between experimental and theoretical data. A similar conclusion was reached from a comparison of curve 2 with the calculation performed in [16] for $M = 13$. Based on the comparison, one can conclude that the increase in density along the shock-heated region in argon when $M = 10$ is primarily associated with radiation cooling.

LITERATURE CITED

1. A. E. Voitenko, "Production of high-velocity gas jets," Dokl. Akad. Nauk SSSR, 158, No. 6, 1278 (1964).
2. T. V. Bazhenova, L. G. Gvozdeva, I. M. Naboko, R. G. Nemkov, Yu. S. Lobastov, and O. A. Predvoditeleva, Shock Waves in Real Gases [in Russian], Nauka, Moscow (1968).
3. H. Mirels, "Limitation on shock-tube test time because of a turbulent boundary layer at the wall," AIAA J., 2, 84 (1964).
4. H. Mirels, "Test time for low-pressure shock tubes," Phys. Fluids, 6, No. 9, 1201 (1963).
5. A. A. Kon'kov, A. P. Ryazin, and A. I. Sokolov, "Two-diaphragm tube for the production of a dense thermal plasma," Teplofiz. Vys. Temp., 12, No. 4, 806 (1974).
6. D. S. Rozhdestvenskii, Papers on Anomalous Dispersion in Metal Vapors [in Russian], Izd. Akad. Nauk SSSR, Moscow (1951).
7. S. G. Zaitsev, E. V. Lazareva, and E. I. Chebotareva," Study of ionized argon behind a shock wave by an interference method," Magnitn. Gidrodinam., No. 3, 86 (1967).
8. A. A. Kon'kov, A. P. Ryazin, and V. S. Rudnev, "Determination of temperature behind a reflected shock wave in air for Mach numbers 10-30," J. Quant. Spectrosc. Radiat. Transfer, 7, No. 2, 339 (1967).
9. P. H. Rose and W. I. Stark, "Stagnation point heat-transfer measurements in dissociated air," J. Aero. Sci., 25, No. 2, 86 (1958).
10. C. W. Allen, Astrophysical Quantities, 2nd ed., Oxford University Press (1963).
11. R. A. Alpher and D. R. White, "Optical interferometry," in: Plasma Diagnostic Techniques (edited by R. H. Huddlestone and S. L. Leonard), Academic Press, (1965).
12. M. P. Bristow and L. L. Glass, "Polarizability of singly ionized argon," Phys. Fluids, 15, No. 11, 2066 (1972).
13. G. I. Kozlov and E. L. Stupitskii, "Calculation of argon state behind an incident shock wave in the range of Mach numbers 20-50 including excitation of multiple ionization and Coulomb interaction," Zh. Prikl. Mekh. Tekh. Fiz., No. 3, 94 (1968).
14. E. Resler, S. C. Lin, and A. Kantrovits, "Production of high-temperature gases in shock tubes," in: Shock Tubes [Russian translation], IL, Moscow (1962).
15. H. Mirels, "Flow nonuniformity in shock tubes operating at maximum test," Phys. Fluids, 9, No. 10, 1907 (1966).
16. V. G. Sevast'yanenko and I. T. Yakubov, "Radiation cooling of gas heat by a strong shock," Opt. Spektrosk., 26, No. 1, 3 (1964).
17. M. McChesney and Z. Al-Attar, "Continuum radiation losses in shock-heated argon," J. Quant. Spectrosc. Radiat. Transfer, 5, No. 4, 533 (1965).